Rotationally induced population inversion between the $B\,^2\Sigma_u^+$ and $X\,^2\Sigma_g^+$ states of N_2^+ exposed to an intense laser pulse

Youyuan Zhang, Erik Lötstedt, and Kaoru Yamanouchi*

Department of Chemistry, School of Science, The University of Tokyo, 7-3-1 Hongo, Bunkyo-ku, Tokyo 113-0033, Japan

(Received 10 December 2019; revised manuscript received 18 March 2020; accepted 8 April 2020; published 7 May 2020)

We investigate the role of the rotational excitation in the coherent and unidirectional $B\,^2\Sigma_u^+$–$X\,^2\Sigma_g^+$ emission of N_2^+ at 391 nm called air lasing generated when N_2 is irradiated with intense femtosecond near-infrared laser pulses at 800 nm. We simulate the time-dependent population transfer process of N_2^+, which is assumed to be generated suddenly in an intense ultrashort laser pulse, by including vibrational and rotational degrees of freedom, and reveal that, when the light field intensity is below $\approx 4 \times 10^{14}$ W cm^{-2}, the population inversion can be achieved in N_2^+ only between rotationally highly excited levels in the vibrational ground ($v' = 0$) state of the $B\,^2\Sigma_u^+$ state and those in the vibrational ground ($v'' = 0$) state of the $X\,^2\Sigma_g^+$ state, so that the lasing at 391 nm is realized even when the total population in the $v' = 0$ state of the electronically excited $B\,^2\Sigma_u^+$ state is not inverted with respect to the total population in the $v'' = 0$ state of the electronic ground $X\,^2\Sigma_g^+$ state.

DOI: 10.1103/PhysRevA.101.053412

I. INTRODUCTION

When intense femtosecond laser pulses are focused in air, unidirectional and coherent radiation called air lasing is generated, originating from the population inversion processes between an electronically excited state and the electronic ground state of N_2 and N_2^+ [1,2]. Among the air-lasing emission lines, the emission at 391 nm from the vibrational ground state in the electronically excited $B\,^2\Sigma_u^+$ state to the vibrational ground state in the electronic ground $X\,^2\Sigma_g^+$ state of N_2^+ [3,4] has attracted much attention in the past years, and a variety of different scenarios have been proposed for the mechanism of the lasing action. For example, the superradiance [5–8], in which a group of excited molecules interact with light collectively and coherently, was proposed as a possible mechanism of the air lasing. As another mechanism, seed amplification induced by a stimulated emission [4,9,10] has been proposed as an emission mechanism.

As for the excitation process, field-induced inelastic recollision [6,11] was proposed for the mechanism of the preparation of N_2^+ in the electronically excited $B\,^2\Sigma_u^+$ state. Later on it was reported that the recollision mechanism could not explain air-lasing phenomenon [12,13]. On the other hand, the postionization optical coupling [4,10] was proposed as a possible mechanism by which the population is inverted between the $B\,^2\Sigma_u^+$ and $X\,^2\Sigma_g^+$ states. By employing a sudden turn-on pulse [4,14], we revealed theoretically that the population inversion can be achieved between the $B\,^2\Sigma_u^+$ state and the $X\,^2\Sigma_g^+$ state so that the air lasing at 391 nm is realized [4,15]. It was shown recently that the effect of molecular alignment [16] as well as the effect of the laser polarization [17] in the air lasing at 391 nm are interpreted well by the postionization optical coupling model with a sudden turn-on laser pulse.

In 2017 [14], we investigated theoretically population transfer in a two-level system exposed to a sudden turn-on pulse by quasistationary Floquet theory [18] and showed that the population transfer processes can be interpreted as adiabatic population transfer from the Floquet states to the field-free excited states. By extending this method so that it can treat a multiple-level system exposed to a sudden turn-on laser pulse, we investigated the population transfer among the three electronic states of N_2^+, i.e., the electronic ground $X\,^2\Sigma_g^+$ state, the first electronically excited $A\,^2\Pi_u$ state, and the second electronically excited $B\,^2\Sigma_u^+$ state, and revealed that the participation of the $A\,^2\Pi_u$ state can reduce the threshold light-field intensity for the population inversion between the vibrational levels in the $B\,^2\Sigma_u^+$ and $X\,^2\Sigma_g^+$ states, and facilitate the lasing action at 391 nm [15].

Recent experimental studies showed that the rotational degrees of freedom need to be taken into account in the interpretation of the lasing at 391 nm. The rotational coherence in the 391-nm lasing was identified through pump-probe measurements [19] and the evidence of the coherent couplings between the rotational levels of the $B\,^2\Sigma_u^+$ state and the rotational levels of the $X\,^2\Sigma_g^+$ state were found by time-resolved spectroscopy [20] and were theoretically interpreted [21]. The rotational excitation was also suggested as a possible mechanism of the population inversion between the $B\,^2\Sigma_u^+$ state and the $X\,^2\Sigma_g^+$ state [22,23]. In Refs. [22,23], through the spectroscopic measurements, it was shown that the population inversion can be achieved between rotational levels in the $B\,^2\Sigma_u^+$ state and those in the $X\,^2\Sigma_g^+$ state when the wavelengths of the excitation laser are 800 [22,24] and 1500 nm [23].

In our previous studies, we interpreted theoretically the population transfer processes of N_2^+ among the three electronic states in an intense ultrashort laser field by taking into account its vibrational degrees of freedom [15,16]. In the present study, by considering the importance of rotation of

*kaoru@chem.s.u-tokyo.ac.jp

N_2^+, we develop our theoretical model for treating the postionization couplings among the three electronic states of N_2^+ by including the rotational degrees of freedom. By carefully adjusting the light field intensity, we reveal that, in a specific light-field intensity range, the population inversion can be achieved in N_2^+ between rotationally highly excited levels in the $B\,^2\Sigma_u^+$ state and those in the $X\,^2\Sigma_g^+$ state, even when the total population in the $v' = 0$ state of the electronically excited $B\,^2\Sigma_u^+$ state is not inverted with respect to the total population in the $v'' = 0$ state of the electronic ground $X\,^2\Sigma_g^+$ state, leading to the rotationally induced lasing at 391 nm.

II. THEORY

The time-dependent population transfer in the N_2^+ system can be described by the time-dependent Schrödinger equation,

$$i\hbar\frac{\partial}{\partial t}\Psi(\mathbf{r},t) = H(t)\Psi(\mathbf{r},t), \tag{1}$$

where $H(t)$ is the Hamiltonian operator. We express the general solution as

$$\Psi(\mathbf{r},t) = \sum_{\alpha=\mathrm{X,A_+,A_-,B}}\sum_{v=0}^{v_{\max}}\sum_{K=0}^{K_{\max}}\sum_{m=-K}^{K} c_{\alpha vKm}(t)\psi_{\alpha vKm}(\mathbf{r}). \tag{2}$$

In Eq. (2), α denotes one of the four lowest-energy electronic states, that is, the $X\,^2\Sigma_g^+$ state, the doubly degenerate $A\,^2\Pi_u$ state (called the A_+ state and A_- state), and the $B\,^2\Sigma_u^+$ state, where v is the vibrational quantum number, K is the angular momentum quantum number of N_2^+, including the electronic orbital angular momentum, m is the projection of the total angular momentum on the space-fixed z axis, and $\mathbf{r}$ is the internuclear separation vector. Even though the spin angular momentum is not considered here, the Hund's case (b) scheme is adopted for the notation of the angular momentum quantum numbers. In the simulation, the maximum vibrational quantum number and the maximum rotational quantum number included in the calculation are denoted as $v_{\max}$ and $K_{\max}$, respectively.

The basis wave function of the Kth rotational state having the quantum number K in the vth vibrational state in the electronic state α, denoted as $\psi_{\alpha vKm}(\mathbf{r})$, has the form of

$$\psi_{\alpha vKm}(\mathbf{r}) = |\alpha\rangle|v\rangle^{\alpha,K}|K,m\rangle^{\alpha}, \tag{3}$$

where $|\alpha\rangle$ is the electronic wave function and $|v\rangle^{\alpha,K}$ is the vibrational basis wave function calculated as the solution of the time-independent Schrödinger equation,

$$H_0^{\mathrm{vib}}|v\rangle^{\alpha,K} = E_{v;\alpha,K}|v\rangle^{\alpha,K}, \tag{4}$$

with the field-free vibrational Hamiltonian H_0^{vib},

$$H_0^{\mathrm{vib}} = -\frac{\hbar^2}{2\mu}\frac{\partial^2}{\partial r^2} + V_\alpha(r) + \frac{K(K+1)-k^2}{2\mu r^2}, \tag{5}$$

where k is the projection of the electronic orbital angular momentum on the molecular axis. In solving Eq. (4), we adopted the finite difference method [25], using the potential energy curves of the $X\,^2\Sigma_g^+$, $A\,^2\Pi_u$, and $B\,^2\Sigma_u^+$ states reported in Refs. [26,27]. The rotational basis function, $|K,m\rangle^\alpha$ is defined as

$$|K,m\rangle^\alpha = \begin{cases} |K,m,0\rangle & \text{when } \alpha = X \text{ or B} \\ (|K,m,1\rangle + |K,m,-1\rangle)/2 & \text{when } \alpha = A_+ \\ (|K,m,1\rangle - |K,m,-1\rangle)/2 & \text{when } \alpha = A_-. \end{cases} \tag{6}$$

In Eq. (6), the rotational wave functions $|K,m,k\rangle$ are defined as [28]

$$|K,m,k\rangle = \frac{1}{\sqrt{2}}\sqrt{(K+m)!(K-m)!(K+k)!(K-k)!(2K+1)} \times \sum_\sigma (-1)^\sigma \frac{[\cos(\theta/2)]^{2K+k-m-2\sigma}[-\sin(\theta/2)]^{m-k+2\sigma}}{\sigma!(K-m-\sigma)!(m-k+\sigma)!(K+k-\sigma)!} e^{im\phi}, \tag{7}$$

where θ is the polar angle and ϕ is the azimuth angle in the polar coordinate system whose z direction is defined as the polarization direction of the laser field and σ starts from the larger of 0 and $(k-m)$ and ends at the smaller of $(K-m)$ and $(K+k)$. For $X\,^2\Sigma_g^+$ and $B\,^2\Sigma_u^+$, $k=0$, and $|K,m,0\rangle$ becomes spherical harmonics. For the degenerate $A\,^2\Pi_u$ state, $k=\pm1$, and the two basis functions, $|K,m\rangle^{A_+}$ and $|K,m\rangle^{A_-}$, constructed as shown in Eq. (6) are symmetric with respect to the transformation of $\theta \to \pi - \theta$ while the wave functions, $|K,m,+1\rangle$ and $|K,m,-1\rangle$, are neither symmetric nor antisymmetric.

The field-free basis set $\{\psi_{\alpha vK}\}$ is orthonormal, and the time-dependent wave function is normalized so that

$$\langle\Psi(t)|\Psi(t)\rangle = \sum_{\alpha=\mathrm{X,A_+,A_-,B}}\sum_{v=0}^{v_{\max}}\sum_{K=0}^{K_{\max}}\sum_{m=-K}^{K}|c_{\alpha vKm}(t)|^2 = 1, \tag{8}$$

is fulfilled, where $P_{\alpha vKm} = |c_{\alpha vKm}(t)|^2$ represents the probability of finding the system in the rotational state with quantum numbers K and m in the vth vibrational state of the electronic state α.

By substituting Eq. (2) into Eq. (1) and multiplying $\psi^*_{\beta v'K'm'}(\mathbf{r})$, representing the basis function of the electronic state β, from left and integrating over $\mathbf{r}$, we obtain

$$i\hbar\frac{d}{dt}c_{\beta v'K'm'}(t) = \sum_{\alpha=\mathrm{X,A_+,A_-,B}}\sum_{v=0}^{v_{\max}}\sum_{K=0}^{K_{\max}}\sum_{m=-K}^{K} c_{\alpha vKm}(t)H_{\beta v'K'm'\alpha vKm}(t), \tag{9}$$

where

$$H_{\beta v'K'm'\alpha vKm}(t) = \int_0^\infty\int_0^\pi\int_0^{2\pi}\psi^*_{\beta v'K'm'}(\mathbf{r})H(t)\psi_{\alpha vKm}(\mathbf{r})dr\sin\theta d\theta d\phi. \tag{10}$$

Under an intense laser field, the total Hamiltonian H of the system interacting with the laser field is written as

$$H(t) = -\frac{\hbar^2}{2\mu}\nabla^2 + V + H_1(t) = H_0 + H_1(t), \tag{11}$$

where μ is the reduced mass of $N_2{}^+$, V is the interatomic potential energy, and H_1 stands for the interaction with the laser field. Consequently, $H_{\beta v'K'm'\alpha vKm}(t)$ becomes

$$H_{\beta v'K'm'\alpha vKm}(t) = (H_0)_{\beta v'K'm'\alpha vKm} + (H_1)_{\beta v'K'm'\alpha vKm}(t), \tag{12}$$

where

$$\begin{aligned}(H_0)_{\beta v'K'm'\alpha vKm} &= \langle\psi_{\beta v'K'm'}|H_0|\psi_{\alpha vKm}\rangle \\ &= \varepsilon_{\alpha vKm}\delta_{\alpha\beta}\delta_{v'v}\delta_{K'K}\delta_{m'm}\end{aligned} \tag{13}$$

and

$$\begin{aligned}(H_1)_{\beta v'K'm'\alpha vKm}(t) &= \langle\psi_{\beta v'K'm'}|H_1(t)|\psi_{\alpha vKm}\rangle \\ &= \langle\psi_{\beta v'K'm'}|D_{\alpha\beta}F_\theta^{\alpha\beta}|\psi_{\alpha vKm}\rangle\mathcal{E}(t).\end{aligned} \tag{14}$$

In Eq. (13), $\varepsilon_{\alpha vKm}$ stands for the eigenenergy of the rotational state $\psi_{\alpha vKm}$ in the vth vibrational state of the electronic state α, and $\mathcal{E}(t)$ in Eq. (14), representing the coupling between rotational states via the transition dipole moment $D_{\alpha\beta}$, stands for the strength of the linearly polarized laser field at time t, defined as

$$\mathcal{E}(t) = \mathcal{E}_0 f(t)\cos(\omega t), \tag{15}$$

where $f(t)$ is an envelope function, ω is the frequency of the laser pulse, and $F_\theta^{\alpha\beta}$ is the angular factor defined as

$$F_\theta^{\alpha\beta} = \cos(\theta)(\delta_{B\alpha}\delta_{X\beta} + \delta_{X\alpha}\delta_{B\beta}) + \sin(\theta)(\delta_{A\alpha}\delta_{X\beta} + \delta_{X\alpha}\delta_{A\beta}). \tag{16}$$

Because the laser field is linearly polarized, $F_\theta^{\alpha\beta}$ does not depend on the azimuth angle ϕ, which means that the quantum number m is conserved during the interaction with the laser field. The rotational transition probability is given by

$$\left|p^{K,m}_{X\beta(\Delta K_\beta)}\right|^2 = |^X\langle K, m|F_\theta^{X\beta}|K + \Delta K_\beta, m\rangle^\beta|^2, \tag{17}$$

for $\beta = B$, $\Delta K_B = \pm 1$, and for $\beta = \mathrm{A}$, $\Delta K_A = \pm 1, 0$. For given K and m,

$$p^{K,m}_{XB(\Delta N_B)} = \begin{cases} \left[\frac{(K-m+1)(K+m+1)}{(2K+1)(2K+3)}\right]^{\frac{1}{2}} & \text{when } \Delta K_B = 1, \\ \left[\frac{(K-m)(K+m)}{(2K+1)(2K-1)}\right]^{\frac{1}{2}} & \text{when } \Delta K_B = -1. \end{cases} \tag{18}$$

$$\begin{aligned} p^{K,m}_{XA(\Delta N_A)} &= K!\sqrt{(K+m)!(K-m)!(K+\Delta K_\mathrm{A}+m)!(K+\Delta K_\mathrm{A}-m)!} \\ &\times \sqrt{(K+\Delta K_A+1)!(K+\Delta K_A-1)!(2K+1)[2(K+\Delta K_A)+1]} \\ &\times \sum_{\sigma=0}^{N-m}\left\{\frac{(-1)^\sigma}{\sigma!(K-m-\sigma)!(m+\sigma)!(K-\sigma)!(2+2N+\Delta K_A)!}\right. \\ &\times \left[\sum_{\sigma'}(-1)^{\sigma'-1}\frac{(1-m+2N+\Delta K_A-\sigma-\sigma')!(m+\sigma+\sigma')!}{\sigma'!(K+\Delta K_A-m-\sigma')!(m-1+\sigma')!(K+\Delta K_A+1-\sigma')!}\right. \\ &\left.\left. + (-1)^{\Delta K_A}\sum_{\sigma_s'}(-1)^{\sigma_s'+1}\frac{(2N-m+\Delta K_A-\sigma-\sigma_s')!(1+m+\sigma+\sigma_s')!}{\sigma_s'!(K+\Delta K_A-m-\sigma_s')!(m+1+\sigma_s')!(K+\Delta K_A-1-\sigma_s')!}\right]\right\}, \end{aligned} \tag{19}$$

where σ' starts from the larger of 0 and $(1-m)$ and ends at $(K+\Delta K_A-m)$, and σ_s' starts from 0 and ends at the smaller of $(K+\Delta K_A-m)$ and $(K+\Delta K_A-1)$.

The envelope function in Eq. (15) is defined as

$$f(t) = e^{-t^2/2\sigma_0^2}, \tag{20}$$

where σ_0 is chosen so that the full-width at half-maximum of the intensity of the laser pulse becomes 28.3 fs.

III. RESULTS AND DISCUSSION

In the simulation of the population transfer among the rotational levels of $N_2{}^+$, we assume the same sudden turn-on laser pulse as that adopted in Ref. [15] with an envelope function defined in Eq. (20) for $t \geqslant 0$. We also assume that the rotational temperature T is $T = 300$ K. The time-dependent total wave function of $N_2{}^+$ ion is expressed as shown in Eq. (2).

The vibrational basis functions and the eigenenergy of the vibrational levels are derived using the potential energy curves of the $X\,^2\Sigma_g^+$, $A\,^2\Pi_u$, and $B\,^2\Sigma_u^+$ electronic states of $N_2{}^+$ given by Refs. [26,27]. The transition dipole moment between $X\,^2\Sigma_g^+$ and $A\,^2\Pi_u$ is perpendicular to the molecular axis, while that between $X\,^2\Sigma_g^+$ and $B\,^2\Sigma_u^+$ is parallel to the molecular axis. The numerical values of these two transition dipole moments are taken from Refs. [26,27].

We solve the time-dependent Schrödinger equation with a sufficiently small time step by assuming that $N_2{}^+$ is prepared in the $X\,^2\Sigma_g^+(v=0)$ state at $t=0$. Using the populations in the rotational levels $|\alpha vK'm\rangle$ at time t obtained from the time propagation of the respective initial states, the time-dependent variation of the populations in the rotational levels is evaluated as the thermal average of the populations in the rotational levels given by

$$p_{\alpha vK'}(t) = \frac{1}{\zeta}\sum_{K=0}^{K_\mathrm{max}}\sum_{m=-K}^{K}\left|c^{X0Km}_{\alpha vK'm'}(t)\right|^2 g_K e^{\frac{-B_{\alpha v}K(K+1)}{k_BT}}, \tag{21}$$

where $c^{X0Km}_{\alpha vK'm'}(t)$ are the time-dependent coefficients obtained from the solution of Eq. (9) using the initial conditions

$c^{X0Km}_{\alpha v K' m'}(t=0) = \delta_{X\alpha}\delta_{0v}\delta_{KK'}\delta_{mm'}$, $B_{\alpha v}$ is the rotational constant, k_B is the Boltzmann constant, g_K is the nuclear spin statistical weight, taking the values of $g_K = 2$ for even K and $g_K = 1$ for odd K, and ζ is the normalization factor given by

$$\zeta = \sum_{K=0}^{K_{\max}} g_K(2K+1)e^{\frac{-B_{\alpha v}K(K+1)}{k_B T}}. \tag{22}$$

The final population after the interaction with the laser pulse is denoted by $P_{\alpha vK}$,

$$P_{\alpha vK} = \lim_{t\to\infty} p_{\alpha vK}(t). \tag{23}$$

A. Rovibronic excitation leading to rotationally inverted population

The relative tunneling ionization probability of N_2, resulting in the creation of the electronic ground $X\,^2\Sigma_g^+$ state of N_2^+ at the laser field intensity of 2×10^{14} W cm^{-2} can be estimated by molecular Ammosov-Delone-Krainov (MO-ADK) theory to be 90% [29], which is much larger than the populations prepared in the $A\,^2\Pi_u$ state (5%) and the $B\,^2\Sigma_u^+$ state (5%). In addition, because the Frank-Condon factor for the ionization from the vibrational ground state of N_2 to the vibrational ground state of N_2^+ is 0.9, we assume for simplicity that N_2^+ generated by the irradiation of an intense laser pulse at $t = 0$ is prepared in the vibrational ground state of the $X\,^2\Sigma_g^+$ state, hereafter referred to as X($v = 0$). In calculating the interaction with the sudden turn-on pulse, the lowest four vibrational levels are included [$v_{\max} = 3$ in Eq. (2)] in all the three electronic states, and the temporal variation of the populations in the respective rotational levels are obtained at a sufficiently small time step of 0.024 fs. Because the effect of the rotational excitation in N_2 induced until just before the ionization on the population distribution of the rotational levels of N_2^+ is not significant, as confirmed numerically in the Appendix, the initial population is assumed to be represented by the Boltzmann distribution at $T = 300$ K, and $K_{\max}$ in Eqs. (21) and (2) is set to be 40.

We perform the numerical simulations with 48 different laser field intensities and examine the variation of the final distributions of the population $P_{\alpha vK}$ of the rotational levels in the $X(v = 0)$, $A(v = 0)$, and $B(v = 0)$ states. The final population $P_{\alpha vK}$ is defined in Eq. (23) as the population after the interaction with the laser pulse. As shown in Fig. 1(a), at the laser field intensity of 2×10^{14} W cm^{-2}, the population inversion is not achieved between the $B\,^2\Sigma_u^+$ state and the $X\,^2\Sigma_g^+$ state, but, as shown in Fig. 1(c), at the laser field intensity of 6×10^{14} W cm^{-2} the population inversion is achieved so that the lasing emission through the R-branch and P-branch transitions can proceed in the entire range of the rotational quantum numbers, showing that the total population inversion is achieved between the $B(v = 0)$ state and the $X(v = 0)$ state, which is consistent with the previous experimental report [23], in which both P-branch and R-branch emission lines are observed at the laser field intensity of 6×10^{14} W cm^{-2}. The zigzag pattern of the population distribution in the rotational levels shown in Fig. 1 reflects the nuclear spin statistical weights of N_2^+ appearing in Eq. (21); that is, $g_K = 2$ for even K rotational levels and $g_K = 1$ for odd K rotational levels.

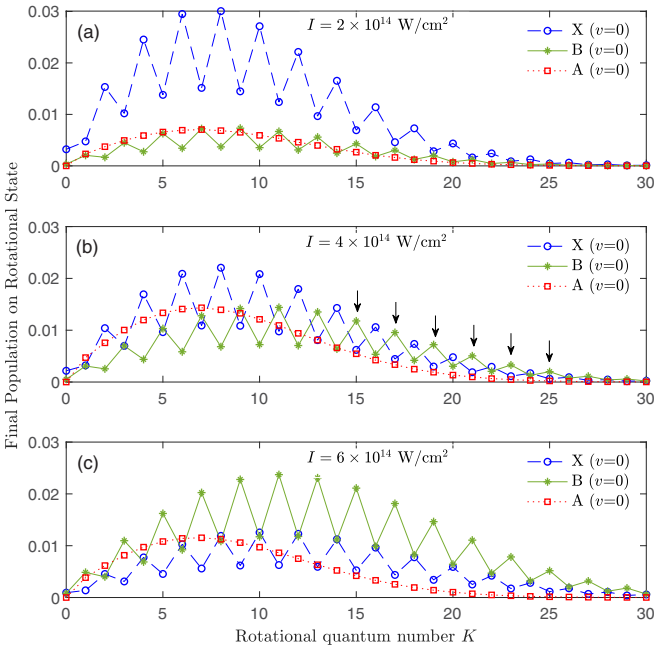

FIG. 1. Final population distribution in the rotational levels of N_2^+ obtained after the interaction with an intense 800-nm laser pulse. The field intensities are set to be (a) 2×10^{14} W cm^{-2}, (b) 4×10^{14} W cm^{-2}, and (c) 6×10^{14} W cm^{-2}. In the calculation, it is assumed that N_2^+ is prepared in the $X\,^2\Sigma_g^+(v = 0)$ state at $t = 0$. For the A state, the sum of the populations in the A_+ and A_- states is shown. The short downward arrows in (b) indicate the rotational levels in the $B\,^2\Sigma_u^+$ state from which the lasing emission occurs via the P-branch transitions to the $X(v = 0)$ state. The label "$\alpha(v = n)$" stands for the nth vibrational state of the α state.

Interestingly, at the intermediate laser field intensity of 4×10^{14} W cm^{-2} as shown in Fig. 1(b), the population inversion between the $B(v = 0)$ state and the $X(v = 0)$ state is achieved only in the rotationally highly excited levels, which was suggested experimentally in Ref. [23]. Indeed, the P-branch emission from $B(v = 0)$ becomes possible when $K' \geqslant 15$ and the R-branch emission from $B(v = 0)$ becomes possible when $K' \geqslant 21$. This theoretical finding can be confirmed experimentally if the light field intensity is chosen appropriately in the intermediate intensity range and the $B(v = 0)$–$X(v = 0)$ emission spectrum is recorded with sufficiently high resolution so that P-branch and R-branch transitions are resolved.

We also find that the rotational population distribution of the $B(v = 0)$ state exhibits the peak at around $K' = 10$. In order that the Boltzmann distribution exhibits a peak at $K' = 10$, the rotational temperature needs to be at 573 K. On the other hand, we find that the rotational population distribution of the $X(v = 0)$ state exhibits a peak at $K' = 8$, corresponding to the rotational temperature at 401 K and that of the $A(v = 0)$ state exhibits a peak at $K' = 7$, which corresponds to the Boltzmann distribution at 302 K.

This discrepancy in the effective rotational temperature in the $B(v = 0)$ state and that in the $X(v = 0)$ state can be ascribed to the difference in the probabilities of the $B\,^2\Sigma_u^+$–$X\,^2\Sigma_g^+$ rovibronic transitions and the probabilities of the $A\,^2\Pi_u$–$X\,^2\Sigma_g^+$ rovibronic transitions. As

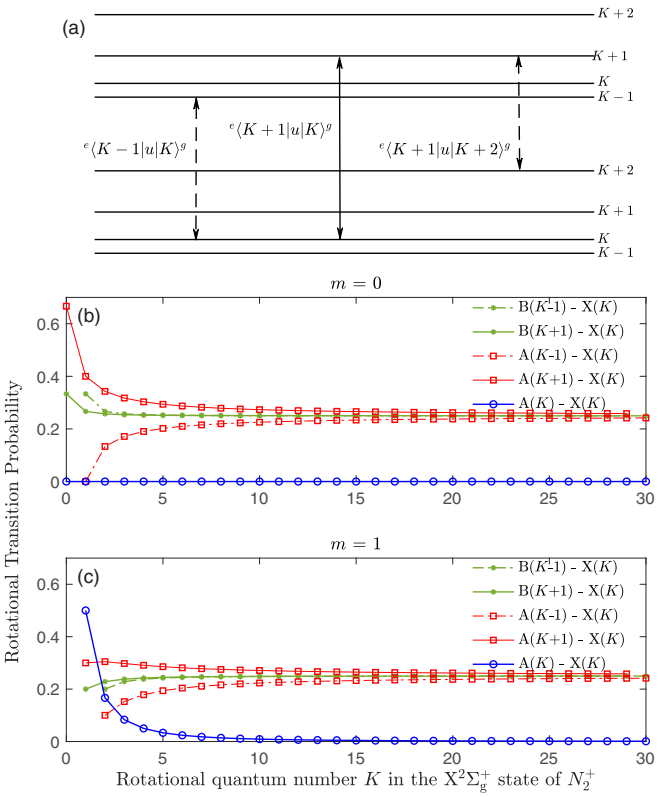

FIG. 2. (a) Illustration of rovibronic population transition. e stands for excited state, and g stands for ground state. Solid double-headed arrow is the R-branch transition and the dashed double-headed arrow stands for the P-branch transition. [(b), (c)] Transition probabilities among the rotational levels of the $X\,^2\Sigma_g^+(v=0)$, $B\,^2\Sigma_u^+(v=0)$, and $A\,^2\Pi_u(v=0)$ states of $N_2{}^+$ plotted as a function of the rotational quantum number K of the $X\,^2\Sigma_g^+$ state of $N_2{}^+$. The projection of the total angular momentum onto the space fixed z axis, m, is chosen to be $m=0$ in panel (b) and it is chosen to be $m=1$ in panel (c).

shown in Eq. (18), the $B\,^2\Sigma_u^+$–$X\,^2\Sigma_g^+$ rovibronic transition probability $|p^{K,m}_{\mathrm{XB}(\Delta N_{\mathrm{B}}=\pm1)}|^2$ is the squared modulus of ${}^{\mathrm{B}}\langle K\pm1,m|\cos\theta|K,m\rangle^{\mathrm{X}}$ and the $A\,^2\Pi_u$–$X\,^2\Sigma_g^+$ rovibronic transition probability $|p^{K,m}_{\mathrm{XA}(\Delta N_{\mathrm{A}}=0,\pm1)}|^2$ is the squared modulus of ${}^{\mathrm{A}}\langle K \text{ or } K\pm1,m|\sin\theta|K,m\rangle^{X}$ according to the rotational transition selection rules of $\Delta K_{\mathrm{B}}=K'-K''=\pm1$ for the $B\,^2\Sigma_u^+$–$X\,^2\Sigma_g^+$ transition and $\Delta K_{\mathrm{A}}=K'-K''=0,\ \pm1$ for the $A\,^2\Pi_u$–$X\,^2\Sigma_g^+$ transition.

The selection rules of the rovibronic transitions are shown in Fig. 2(a), where $|^e\langle K+1|u|K\rangle^g|^2$ stands for the transition probability from the K level in the electronic ground $X\,^2\Sigma_g^+$ state to the $K+1$ level in electronically excited state, where u is $\cos\theta$ for the $B\,^2\Sigma_u^+$–$X\,^2\Sigma_g^+$ transition and $\sin\theta$ for the $A\,^2\Pi_u$–$X\,^2\Sigma_g^+$ transition.

As shown in Figs. 2(b) and 2(c), for the $B\,^2\Sigma_u^+$–$X\,^2\Sigma_g^+$ transition, the probability of the R-branch transition ($\Delta K_{\mathrm{B}}=1$) and that of the P-branch transition ($\Delta K_{\mathrm{B}}=-1$) are almost the same, that is, $|p^{K,m}_{XB(\Delta N_{\mathrm{B}}=1)}|^2\sim|p^{K,m}_{XB(\Delta N_B)=-1}|^2$. This means that the population in the K level in the $X\,^2\Sigma_g^+$ state can be transferred to the higher and lower rotational levels in the $B\,^2\Sigma_u^+$ state with almost equal probabilities and that transitions to the rotational states with large K in the $B\,^2\Sigma_u^+$ state can become populated by a sequence of transitions $X(K)\rightarrow B(K+1)\rightarrow X(K+2)\rightarrow B(K+3)\ldots$.

On the other hand, for the $A\,^2\Pi_u$–$X\,^2\Sigma_g^+$ transition, the probability of the R-branch transition ($\Delta K_A=1$) is always larger than that of the P-branch transition ($\Delta K_A=-1$), that is, $|p^{K,m}_{XA(\Delta N_A=1)}|^2>|p^{K,m}_{XA(\Delta N_A)=-1}|^2$, which means that the probability $|^e\langle K+1|u|K\rangle^g|^2$ represented by the solid double-headed arrow is larger than the probabilities $|^e\langle K-1|u|K\rangle^g|^2$ and $|^e\langle K+1|u|K+2\rangle^g|^2$ represented by the dash double-headed arrows shown in Fig. 2(a) and that the $A\,^2\Pi_u$–$X\,^2\Sigma_g^+$ transition starting from a certain rotational level K preferentially proceeds along the solid line in Fig. 2(a), that is, $X(K)\rightarrow A(K+1)\rightarrow X(K)\ldots$, resulting in the suppression of the population transfer to the higher K levels. In addition, the Q-branch transition ($\Delta K=0$) of the $A\,^2\Pi_u$–$X\,^2\Sigma_g^+$ transition does not transfer the population to the higher or lower K levels.

Because the $X\,^2\Sigma_g^+$ state is coupled with the $B\,^2\Sigma_u^+$ and $X\,^2\Sigma_g^+$ states, the rotational population distributions in $X\,^2\Sigma_g^+$ states is influenced by the $B\,^2\Sigma_u^+$–$X\,^2\Sigma_g^+$ rovibronic transitions, having a tendency to promote the population transfer to the higher lying rotational levels, as well as by the $A\,^2\Pi_u$–$X\,^2\Sigma_g^+$ rovibronic transitions, having a tendency to suppress the population transfer to higher lying rotational levels, the rotational temperature of the $X\,^2\Sigma_g^+$ state is smaller than that of the $B\,^2\Sigma_u^+$ state and larger than that of the $A\,^2\Pi_u$ state.

B. Dependence on the laser field intensity

In order to examine the mechanism of the population inversion between the $B\,^2\Sigma_u^+$ and $X\,^2\Sigma_g^+$ state at the high rotational quantum numbers, we calculate the rotational distributions in the three electronic states as a function of the laser field intensity in the range between 1×10^{14} and 7×10^{14} W cm^{-2}. In the simulation, the wavelength and FWHM of the laser pulse are fixed at 800 nm and 28.3 fs, and the population distributions in the rotational levels in the three electronic state of $N_2{}^+$ after the interaction with the laser pulse are calculated.

In Fig. 3, the population difference between the rotational level of the $B(v=0)$ state having the rotational quantum number K and the rotational level of the $X(v=0)$ state having the rotational quantum number $K+1$ defined as

$$\Delta P_{\mathrm{rot},K}=P_{B0(K)}-P_{X0(K+1)} \tag{24}$$

is plotted as a function of the laser field intensity for the K values in the range between 0 and $K_{\max}-1$. If $\Delta P_{\mathrm{rot},K}$ becomes positive, the population inversion is realized, and consequently, the P-branch lasing emission at 391 nm can be generated.

As shown in Fig. 3, the threshold K value beyond which the population inversion occurs, which is referred to as $K_{\mathrm{threshold}}$, decreases as the laser field intensity increases. Indeed, $K_{\mathrm{threshold}}=21$, at $I=3\times10^{14}$ W cm^{-2}, $K_{\mathrm{threshold}}=14$ at $I=4\times10^{14}$ W cm^{-2}, and $K_{\mathrm{threshold}}=11$ at $I=4.5\times10^{14}$ W cm^{-2}. It can be said that, as long as the laser field intensity is weaker than $\approx4.5\times10^{14}$ W cm^{-2}, the population

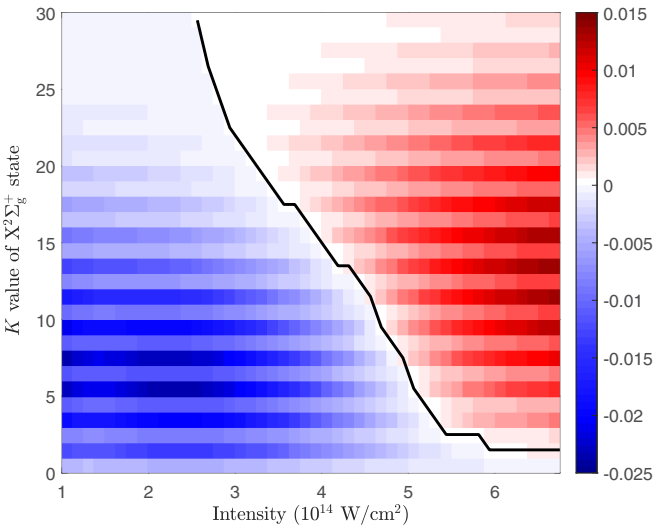

FIG. 3. Final population difference between the rotational level of the $B(v=0)$ state of N_2^+ having the rotational quantum number K and the rotational level of the $X(v=0)$ state having the rotational quantum number $K+1$ after the interaction with an intense ultrashort near-IR (28.3-fs, 800-nm) laser pulse in the intensity range of 1×10^{14}–7×10^{14} W cm^{-2}. The black solid zigzag line represents the threshold rotational quantum number, $N_{\text{threshold}}$, as a function of the laser field intensity. The initial population distribution in the rotational levels of $X(v=0)$ is assumed to have the Boltzmann distribution at 300 K.

inversion is achieved only in the rotationally highly excited region. When the laser field intensity is larger than 4.44×10^{14} W cm^{-2} the population inversion is achieved in the entire range of the rotational quantum number. This is the situation that we call normally the population inversion by implicitly neglecting the rotational degrees of freedom. In our previous study [15], when the alignment angle θ_a of the N-N molecular axis of N_2^+ and the laser polarization direction is set to be $\theta_a=45^\circ$, the population inversion between the $B(v=0)$ state and the $X(v=0)$ state is achieved at the laser field intensity of 2×10^{14} W cm^{-2}. In order to examine if this model in which the alignment angle θ_a is fixed with respect to the laser polarization direction is rationalized, we calculate the population distribution in the rotational levels at a given laser field intensity at different alignment angles in the range of $0<\theta_a<\pi$ at the intervals of 0.5° and take an average over the alignment angles to derive the mean population distribution. After repeating this calculation at different laser field intensities, we find the threshold field intensity for the population inversion is 4.47×10^{14} W cm^{-2}, which is consistent with the threshold field intensity of 4.44×10^{14} W cm^{-2} obtained in the present study, in which the rotational degree of freedom is explicitly taken into account.

IV. CONCLUSION

By explicitly treating the rotational degrees of freedom, we have solved the time-dependent Schrödinger equation to simulate the population transfer processes among the vibrational levels of the $B\,^2\Sigma_u^+$, $A\,^2\Pi_u$, and $X\,^2\Sigma_g^+$ states of N_2^+ exposed to an ultrashort (28.3 fs) intense near-infrared (near-IR; 800-nm) laser field using the model in which N_2^+ interacts with a sudden turn-on laser field. On the basis of the dependences of the population transfer processes on the laser field intensity, we have revealed that the $B\,^2\Sigma_u^+$ state is more rotationally excited than the $X\,^2\Sigma_g^+$ state and the $A\,^2\Pi_u$ state because of the difference between the rotational selection rules and the difference between the transition probabilities of the $B\,^2\Sigma_u^+$–$X\,^2\Sigma_g^+$ and those of the $A\,^2\Pi_u$–$X\,^2\Sigma_g^+$ transition and that, as long as the light-field intensity is weaker than $\sim4.5\times10^{14}$ Wcm^{-2}, the population inversion can be achieved in N_2^+ only between rotationally highly excited levels in the $B\,^2\Sigma_u^+$ state and those in the $X\,^2\Sigma_g^+$ state, leading to the rotationally induced lasing at 391 nm, even though the total population in the $B(v'=0)$ state is not inverted with respect to the total population in the $X(v''=0)$ state.

We have presented a comprehensive model of the strong-field excitation processes in N_2^+ created by an intense laser field, including the electronic, vibrational, and rotational degrees of freedom. By adopting the present theoretical model of the strong-field excitation processes in N_2^+ created by an intense laser field, in which the electronic, vibrational, and rotational degrees of freedom are included, we will be able to simulate the theoretically the role of the electronic, vibrational, and rotational dynamics of N_2^+ in the air lasing [30].

ACKNOWLEDGMENTS

This research was supported by JSPS KAKENHI Grants No. JP15K17805 and No. JP15H05696.

APPENDIX: THE EFFECT OF ROTATIONAL PRE-EXCITATION OF N_2 BEFORE THE IONIZATION

In order to examine the effect of the rotational excitation of neutral N_2 occurring within a femtosecond laser pulse until the timing of the ionization, we solve the time-dependent Schrödinger equation of a rigid rotor [16],

$$i\hbar\frac{\partial}{\partial t}\Phi(\theta,\phi,t)=\left[H_{\text{rot}}-\frac{1}{4}\Delta\alpha\mathcal{E}_0^2f^2(t)\cos^2\theta\right]\Phi(\theta,\phi,t), \tag{A1}$$

where H_{rot} is the field-free rigid-rotor Hamiltonian, $\Delta\alpha$ is the anisotropy of the polarizability of N_2, and $\Phi(\theta,\phi,t)$ is the rotational wave packet, which is defined as

$$\Phi(\theta,\phi,t)=\frac{e^{im\phi}}{\sqrt{2\pi}}\sum_{K=0}^{K_{\max}}C_{Km}(t)|K,m\rangle^{N_2}, \tag{A2}$$

using the normalized associated Legendre functions, $|K,m\rangle^{N_2}$. In the simulation, $\Delta\alpha=0.71$ Å^3 [31] and the rotational constant of $B=1.9895$ cm^{-1} [32] are adopted.

We perform calculations by starting with the respective rotational states of N_2 from $t=-50$ fs until $t=0$, and the resulting coherent rotational state of the rigid rotor is taken as the initial state for the simulation of N_2^+ which starts interacting with the sudden turn-on pulse at

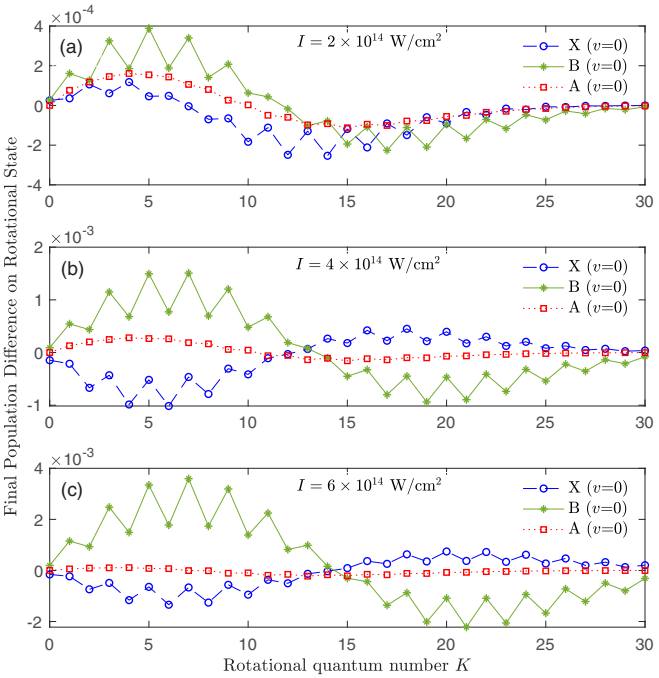

FIG. 4. The difference in the final population distributions obtained when the rotational excitation of neutral N_2 in an intense 800-nm laser field during the period of the earlier half of the Gaussian envelope between $t = -50$ fs and $t = 0$ fs and those obtained when no rotational pre-excitation of neutral N_2 is considered. The field intensities at $t = 0$ are set to be (a) 2×10^{14} W cm^{-2}, (b) 4×10^{14} W cm^{-2}, and (c) 6×10^{14} W cm^{-2}. In the calculation, it is assumed that N_2^+ is prepared in the $X\,^2\Sigma_g^+(v = 0)$ state at $t = 0$. For the A state, the sum of the populations in the A_+ and A_- states is shown. The label "$\alpha(v = n)$" stands for the nth vibrational state of the α state.

$t = 0$. The final rotational population distribution of N_2^+ is obtained by the thermal averaging using the Boltzmann distribution of the initial rotational states of N_2 at $T = 300$ K.

The resultant rotational distributions are found to be very close to those presented in Fig. 1. For example, at 4×10^{14} W cm^{-2}, the population differences in the respective rotational levels are found to be only less than 0.20 % and the population differences in the respective vibrational levels obtained by the summation over the K and m quantum numbers are all less than 0.26%. Therefore, the differences are taken and are expanded as shown in Fig. 4. It can be seen clearly in Figs. 4(b) and 4(c) that the rotational distributions in the $B\,^2\Sigma_u^+$ state have a tendency to be shifted toward the lower K values while the rotational distribution in the $X\,^2\Sigma_g^+$ state have a tendency to be shifted toward the higher K values. It can also be seen in these three subfigures [Figs. 4(a)–4(c)] that the rotational distributions in the $A\,^2\Pi_u$ state are less influenced by the rotational pre-excitation in neutral N_2.

When the rotational distributions are expressed using the Boltzmann temperature, the rotational temperatures of the $X\,^2\Sigma_g^+$, $A\,^2\Pi_u$, and $B\,^2\Sigma_u^+$ states at 4×10^{14} W cm^{-2} are obtained to be 424, 295, and 505 K, respectively. On the other hand, the rotational temperatures of the $X\,^2\Sigma_g^+$, $A\,^2\Pi_u$, and $B\,^2\Sigma_u^+$ states obtained when the rotational pre-excitation in neutral N_2 is not considered are 401, 302, and 573 K, respectively. It is true that the rotational excitation in the $B\,^2\Sigma_u^+$ state of N_2^+ is slightly suppressed and that in the $X\,^2\Sigma_g^+$ state of N_2^+ is slightly enhanced, but the variations are so small that the population inversion only in the rotationally highly excited levels is still achieved between the $B(v = 0)$ state and the $X(v = 0)$ state.

[1] Q. Luo, W. Liu, and S. Chin, Lasing action in air induced by ultra-fast laser filamentation, App. Phys. B **76**, 337 (2003).

[2] A. Dogariu, J. B. Michael, M. O. Scully, and R. B. Miles, High-gain backward lasing in air, Science **331**, 442 (2011).

[3] J. Yao, B. Zeng, H. Xu, G. Li, W. Chu, J. Ni, H. Zhang, S. L. Chin, Y. Cheng, and Z. Xu, High-brightness switchable multiwavelength remote laser in air, Phys. Rev. A **84**, 051802 (2011).

[4] H. Xu, E. Lötstedt, A. Iwasaki, and K. Yamanouchi, Sub-10-fs population inversion in N_2^+ in air lasing through multiple state coupling, Nat. Commun. **6**, 8347 (2015).

[5] G. Li, C. Jing, B. Zeng, H. Xie, J. Yao, W. Chu, J. Ni, H. Zhang, H. Xu, Y. Cheng, and Z. Xu, Signature of superradiance from a nitrogen-gas plasma channel produced by strong-field ionization, Phys. Rev. A **89**, 033833 (2014).

[6] Y. Liu, P. Ding, G. Lambert, A. Houard, V. Tikhonchuk, and A. Mysyrowicz, Recollision-Induced Superradiance of Ionized Nitrogen Molecules, Phys. Rev. Lett. **115**, 133203 (2015).

[7] X. Zhong, Z. Miao, L. Zhang, Q. Liang, M. Lei, H. Jiang, Y. Liu, Q. Gong, and C. Wu, Vibrational and electronic excitation of ionized nitrogen molecules in intense laser fields, Phys. Rev. A **96**, 043422 (2017).

[8] X. Zhong, Z. Miao, L. Zhang, H. Jiang, Y. Liu, Q. Gong, and C. Wu, Optimizing the 391-nm lasing intensity from ionized nitrogen molecules in 800-nm femtosecond laser fields, Phys. Rev. A **97**, 033409 (2018).

[9] J. Ni, W. Chu, C. Jing, H. Zhang, B. Zeng, J. Yao, G. Li, H. Xie, C. Zhang, H. Xu, S.-L. Chin, Y. Cheng, and Z. Xu, Identification of the physical mechanism of generation of coherent N_2^+ emissions in air by femtosecond laser excitation, Opt. Express **21**, 8746 (2013).

[10] J. Yao, S. Jiang, W. Chu, B. Zeng, C. Wu, R. Lu, Z. Li, H. Xie, G. Li, C. Yu, Z. Wang, H. Jiang, Q. Gong, and Y. Cheng, Population Redistribution Among Multiple Electronic States of Molecular Nitrogen Ions in Strong Laser Fields, Phys. Rev. Lett. **116**, 143007 (2016).

[11] V. T. Tikhonchuk, J.-F. Tremblay-Bugeaud, Y. Liu, A. Houard, and A. Mysyrowicz, Excitation of nitrogen molecular ions in a strong laser field by electron recollisions, Eur. Phys. J. D **71**, 292 (2017).

[12] M. Britton, P. Laferrière, D. H. Ko, Z. Li, F. Kong, G. Brown, A. Naumov, C. Zhang, L. Arissian, and P. B. Corkum, Testing the Role of Recollision in N_2^+ Air Lasing, Phys. Rev. Lett. **120**, 133208 (2018).

[13] H. Li, Q. Song, J. Yao, Z. Liu, J. Chen, B. Xu, K. Lin, J. Qiang, B. He, H. Xu, Y. Cheng, H. Zeng, and J. Wu, Air lasing from singly ionized N_2 driven by bicircular two-color fields, Phys. Rev. A **99**, 053413 (2019).

[14] Y. Zhang, E. Lötstedt, and K. Yamanouchi, Population inversion in a strongly driven two-level system at far-off resonance, J. Phys. B: At., Mol. Opt. Phys. **50**, 185603 (2017).

[15] Y. Zhang, E. Lötstedt, and K. Yamanouchi, Mechanism of population inversion in laser-driven $N_2{}^+$, J. Phys. B: At., Mol. Opt. Phys. **52**, 055401 (2019).

[16] H. Xu, E. Lötstedt, T. Ando, A. Iwasaki, and K. Yamanouchi, Alignment-dependent population inversion in $N_2{}^+$ in intense few-cycle laser fields, Phys. Rev. A **96**, 041401 (2017).

[17] H. Li, M. Hou, H. Zang, Y. Fu, E. Lötstedt, T. Ando, A. Iwasaki, K. Yamanouchi, and H. Xu, Significant Enhancement of N_2^+ Lasing by Polarization-Modulated Ultrashort Laser Pulses, Phys. Rev. Lett. **122**, 013202 (2019).

[18] I. Maruyama, T. Sako, and K. Yamanouchi, Time-dependent nuclear wavepacket dynamics of H_2^+ by quasi-stationary Floquet approach, J. Phys. B **37**, 3919 (2004).

[19] H. Zhang, C. Jing, J. Yao, G. Li, B. Zeng, W. Chu, J. Ni, H. Xie, H. Xu, S. L. Chin, K. Yamanouchi, Y. Cheng, and Z. Xu, Rotational Coherence Encoded in an "Air-Laser" Spectrum of Nitrogen Molecular Ions in an Intense Laser Field, Phys. Rev. X **3**, 041009 (2013).

[20] B. Zeng, W. Chu, G. Li, J. Yao, H. Zhang, J. Ni, C. Jing, H. Xie, and Y. Cheng, Real-time observation of dynamics in rotational molecular wave packets by use of air-laser spectroscopy, Phys. Rev. A **89**, 042508 (2014).

[21] H. Xie, B. Zeng, G. Li, W. Chu, H. Zhang, C. Jing, J. Yao, J. Ni, Z. Wang, Z. Li, and Y. Cheng, Coupling of N_2^+ rotational states in an air laser from tunnel-ionized nitrogen molecules, Phys. Rev. A **90**, 042504 (2014).

[22] M. Lei, C. Wu, A. Zhang, Q. Gong, and H. Jiang, Population inversion in the rotational levels of the superradiant N_2^+ pumped by femtosecond laser pulses, Opt. Express **25**, 4535 (2017).

[23] A. Azarm, P. Corkum, and P. Polynkin, Optical gain in rotationally excited nitrogen molecular ions, Phys. Rev. A **96**, 051401 (2017).

[24] W. Zheng, Z. Miao, L. Zhang, Y. Wang, C. Dai, A. Zhang, H. Jiang, Q. Gong, and C. Wu, Enhanced coherent emission from ionized nitrogen molecules by femtosecond laser pulses, J. Phys. Chem. Lett. **10**, 6598 (2019).

[25] R. J. LeVeque, *Finite Difference Methods for Ordinary and Partial Differential Equations* (Society for Industrial and Applied Mathematics, Philadelphia, 2007).

[26] S. R. Langhoff, C. W. Bauschlicher, and H. Partridge, Theoretical study of the N_2^+ Meinel system, J. Chem. Phys. **87**, 4716 (1987).

[27] S. R. Langhoff and C. W. Bauschlicher Jr., Theoretical study of the first and second negative systems of N_2^+, J. Chem. Phys. **88**, 329 (1988).

[28] J. M. Brown and A. Carrington, *Rotational Spectroscopy of Diatomic Molecules*, Cambridge Molecular Science (Cambridge University Press, Cambridge, UK, 2003).

[29] S.-F. Zhao, C. Jin, A.-T. Le, T. F. Jiang, and C. D. Lin, Determination of structure parameters in strong-field tunneling ionization theory of molecules, Phys. Rev. A **81**, 033423 (2010).

[30] T. Ando, E. Lötstedt, A. Iwasaki, H. Li, Y. Fu, S. Wang, H. Xu, and K. Yamanouchi, Rotational, Vibrational, and Electronic Modulations in N_2^+ Lasing at 391 nm: Evidence of Coherent $B^2\Sigma_u^+ - X^2\Sigma_g^+ - A^2\Pi_u$ Coupling, Phys. Rev. Lett. **123**, 203201 (2019).

[31] P. J. Bruna and F. Grein, The $A^2\Pi_u$ state of N_2^+: Electric properties, fine and hyperfine coupling constants, and magnetic moments (g-factors): A theoretical study, J. Mol. Spectrosc. **250**, 75 (2008).

[32] A. Lofthus and P. H. Krupenie, The spectrum of molecular nitrogen, J. Phys. Chem. Ref. Data **6**, 113 (1977).